ELSEVIER

Probing for dynamics of dark energy and curvature of universe with latest cosmological observations

Gong-Bo Zhao [a,*], Jun-Qing Xia [a], Hong Li [b], Charling Tao [c], Jean-Marc Virey [d], Zong-Hong Zhu [e], Xinmin Zhang [a]

[a] *Institute of High Energy Physics, Chinese Academy of Science, P.O. Box 918-4, Beijing 100049, PR China*
[b] *Department of Astronomy, School of Physics, Peking University, Beijing 100871, PR China*
[c] *Centre de Physique des Particules de Marseille, CNRS/IN2P3-Luminy and Université de la Méditerranée, Case 907, F-13288 Marseille Cedex 9, France*
[d] *Centre de Physique Théorique, CNRS-Luminy and Université de Provence, Case 907, F-13288 Marseille Cedex 9, France*
[e] *Department of Astronomy, Beijing Normal University, Beijing 100875, PR China*

Received 4 January 2007; received in revised form 21 February 2007; accepted 25 February 2007

Available online 13 March 2007

Editor: T. Yanagida

Abstract

We use the newly released 182 type Ia supernova data combined with the third-year Wilkinson Microwave Anisotropic Probe data (WMAP3) and large scale structure (LSS) information including SDSS and 2dFGRS to constrain the dark energy equation of state (EoS) as well as the curvature of universe Ω_K. Using the full dataset of Cosmic Microwave Background (CMB) and LSS rather than the shift parameter and linear growth factor, we make a Markov Chain Monte Carlo (MCMC) global fit, while paying particular attention to the dark energy perturbation. Parameterizing the EoS as $w_{DE}(a) = w_0 + w_1(1-a)$, we find the best fit of (w_0, w_1) is $(-1.053, 0.944)$ and for $w_{DE}(a) = w_0 + w_1 \sin(\frac{3}{2}\pi \ln(a))$, the best fit for (w_0, w_1) is $(-1.614, -1.046)$. We find that a flat universe is a good approximation, namely, $|\Omega_K| > 0.06$ has been excluded by 2σ yet the inclusion of Ω_K can affect the measurement of DE parameters owing to their correlation and the present systematic effects of SNIa measurements.

1. Introduction

Dark energy (DE), the very power to drive universe's acceleration, is one of the most important issues in modern cosmology. Its existence was firstly revealed by the measurement of the relationship between redshift z and luminosity distance d_L of type Ia supernova (SN Ia) [1]. Dark energy encodes its mystery in its equation of state (EoS) defined as the ratio of pressure over energy density thus DE models can be classified in terms of EoS [2].

The simplest candidate of dark energy is the cosmological constant (CC) whose EoS remains -1. Favored by current astronomical observations as it is, CC suffers from severe the-

oretical drawbacks such as the fine-tunning and coincidence problem [3]. Alternative DE models with rolling scalar field, such as quintessence [4], phantom [5], k-essence [6], etc. have been studied. The EoS of these models varies with cosmic time either above -1 or below -1 during evolution but the statement of "No-Go" theorem forbids it to cross the -1 boundary [7]. Models where gravity is modified can also give these observed effects.

Given our ignorance of the nature of dark energy, constraining the evolution of DE the EoS by cosmological observations is of great significance. Various methods have been used to constrain DE including parametric fitting [8–10], non-parametric reconstruction [11], etc. Interestingly, there exists some hint that the EoS of DE has crossed over -1 at least once from current observations [9,11–13], which greatly challenges the above mentioned dark energy models, albeit the evidence is still marred by systematic effects. Quintom, whose EoS can

---

smoothly cross -1 [14], has attracted a lot of attention in the literature since its invention [15]. There have been many efforts in quintom model building, for example, double-scalar-field realization [14,16], a single scalar field with high derivative [17], vector fields [18] and so forth.

A special and interesting example of quintom is oscillating quintom, whose EoS oscillates with time and crosses -1 many times. The oscillating behavior in the EoS leads to oscillations in the Hubble constant and a recurrent universe. Oscillating quintom is physically well motivated, since this scenario, to some extent, unifies early inflation and the current acceleration of the universe [19]. In Ref. [20], we have presented some preliminary studies on oscillating quintom.

The nature of dark energy is a dominant factor of the fate of our universe. Another critical point is the curvature of universe, Ω_K, albeit small, it will affect the probing of dark energy. We concentrate, in this Letter, on the correlation between Ω_K and the dark energy parameters.[1]

We use the newly released 182 SN Ia "Gold sample" (SN182) [24] combined with WMAP3 [25][2] and LSS information to constrain the evolution of the DE EoS and the curvature of universe. For DE EoS, we choose two parameterizations as in (1) and (2) and we will address our motivation for such a choice in the next section. In our study, we treat the curvature of the universe Ω_K as a free parameter rather than simply assuming a flat universe and make a Markov Chain Monte Carlo (MCMC) global fit based on Bayesian statistics. Paying particular attention to the dark energy perturbation especially when EoS crosses -1 [8], we find the latest observations mildly favor quintom model however ΛCDM remains a good fit. We have also found that the inclusion of Ω_K can affect the determination of DE parameters significantly due to their correlation.

We structure this Letter as follows: after this introductory part, we propose our method and define the data set used in Section 2. In Section 3 we present our results and end up with discussion and comments.

2. Method and data

To study the dynamical behavior of dark energy, we choose two kinds of parametrization of dark energy equation of state:

$$(I) \quad w_{\mathrm{DE}}(a) = w_0 + w_1(1-a), \tag{1}$$

$$(II) \quad w_{\mathrm{DE}}(a) = w_0 + w_1 \sin\big(w_2 \ln(a)\big), \tag{2}$$

where a is the scale factor, w_0 denotes the EoS at present epoch and w_1 and w_2 characterize the time evolution of DE. Parametrization (I) is the most popular in literature since w_1 simply equals to $-dw_{\mathrm{DE}}(a)/da$, which is the time derivative of $w_{\mathrm{DE}}(a)$ [26]. Thus it is straightforward to study the dynamical behavior of DE. The physical motivation of parametrization (II) is oscillating quintom. From (2) we can see at low redshift,

(II) takes a form similar to (I). At medium and high redshift, the EoS keeps oscillating.

From the latest SN Ia paper [24], one can find some hint of oscillating behavior of the EoS in their Fig. 10 where they use a quartic polynomial fit. Our sine function has the advantage of preserving the oscillating feature of the EoS at high redshift measured by the CMB data. For simplicity and focus on the study at lower redshift, we set w_2 to be $\frac{3}{2}\pi$ in order to allow the EoS to evolve more than one period within the redshift range of 0 to 2 where SN data are most robust.

When using the MCMC global fitting strategy to constrain cosmological parameters, it is crucial to include dark energy perturbation. This issue has been realized by many researchers including the WMAP group [7,8,25,27]. However one cannot handle the dark energy perturbation when the parameterized EoS crosses -1 based on quintessence, phantom, k-essence and other non-crossing models. By virtue of quintom, the perturbation at the crossing points is continuous, thus we have proposed a sophisticated technique to treat dark energy perturbation in the whole parameter space, say, EoS > -1, < -1 and at the crossing pivots. For details of this method, we refer the readers to our previous companion paper [7,8].

In this study, we have modified the publicly available Markov Chain Monte Carlo package CAMB/CosmoMC [28] to include the dark energy perturbation when the equation of state crosses -1.

The dark energy EoS and curvature of the universe Ω_K can affect the determination of the geometry of our universe thus DE parameters are correlated with Ω_K. Therefore, in our study, we relax the curvature of universe Ω_K as a free parameter rather than simply assuming a flat universe. We assume purely adiabatic initial conditions and set our most general parameter space as:

$$\mathbf{P} \equiv \big(\omega_b, \omega_c, \Theta_s, \tau, \Omega_K, w_0, w_1, n_s, \ln(10^{10}A_s)\big), \tag{3}$$

where $\omega_b \equiv \Omega_b h^2$ and $\omega_c \equiv \Omega_c h^2$ are the physical baryon and cold dark matter densities relative to the critical density, Θ_s is the ratio (multiplied by 100) of the sound horizon to the angular diameter distance at decoupling, τ is the optical depth to re-ionization, $\Omega_K \equiv 1 - \Omega_m - \Omega_{\mathrm{DE}}$ is the spatial curvature, w_0, w_1 portray the dynamical feature of dark energy as illustrated in (1) and (2). A_s and n_s characterize the primordial scalar power spectrum. For the pivot of the primordial spectrum we set $k_{s0} = 0.05\ \mathrm{Mpc}^{-1}$. Furthermore, we make use of the Hubble Space Telescope (HST) measurement of the Hubble parameter $H_0 \equiv 100\ h\,\mathrm{km\,s}^{-1}\,\mathrm{Mpc}^{-1}$ [29] by multiplying the likelihood by a Gaussian likelihood function centered around $h = 0.72$ and with a standard deviation $\sigma = 0.08$. We also impose a weak Gaussian prior on the baryon density $\Omega_b h^2 = 0.022 \pm 0.002$ (1σ) from big bang nucleosynthesis [30]. The weak priors we take are as follows: $\tau < 0.8$, $0.5 < n_s < 1.5$, $-0.3 < \Omega_K < 0.3$, $-3 < w_0 < 3$, $-5 < w_1 < 5$[3] and a cosmic age tophat prior $10\ \mathrm{Gyr} < t_0 < 20\ \mathrm{Gyr}$.

---

[1] This correlation is of significance as pointed out by [23]. Further, other cosmological parameters also affect the probing of dark energy, such as neutrino mass [21] and inflationary parameters [22].

[2] Available at http://lambda.gsfc.nasa.gov/product/map/current/.

---

[3] We set the prior of w_0 and w_1 broad enough to ensure the EoS can evolve in the whole parameter space.

In our calculations, we have taken the total likelihood to be the products of the separate likelihoods $\mathcal{L}$ of CMB, LSS and SNIa. In other words, defining $\chi^2 \equiv -2 \log \mathcal{L}$, we get

$$\chi^2_{\text{total}} = \chi^2_{\text{CMB}} + \chi^2_{\text{LSS}} + \chi^2_{\text{SNIa}}. \tag{4}$$

If the likelihood function is exactly Gaussian, χ^2 coincides with the usual definition of χ^2 up to an additive constant corresponding to the logarithm of the normalization factor of $\mathcal{L}$. In the calculation of the likelihood from SNIa we have marginalized over the nuisance parameter [31]. The supernova data we use are the "gold" set of 182 SNIa recently published by Riess et al. in Ref. [24]. In the computation of CMB we have used the full dataset of the WMAP3 data with the routine for computing the likelihood supplied by the WMAP team [25]. For LSS information, we have used the 3D power spectrum of galaxies from the SDSS [32] and 2dFGRS [33]. To be conservative but more robust, in the fittings to the 3D power spectrum of galaxies from the SDSS, we have used the first 14 bins only, which are supposed to be well within the linear regime [34]. There are some other observations which are potentially important to constrain the parameters, such as the baryon acoustic oscillations (BAO) information in the SDSS LRG sample [35] which is a powerful "standard ruler" measuring the angular diameter distance to $z = 0.35$. In order to be comparable with the relevant results supplied by the WMAP team [25] we do not use these information in our analysis.

For each regular calculation, we run six independent chains comprising 150 000–300 000 chain elements and spend thousands of CPU hours to calculate on a cluster. The average acceptance rate is about 40%. We discard the first 30% chain elements to be the "burn-in" process, test the convergence of the chains by Gelman and Rubin criteria [36] and find $R - 1$ of order 0.01, which is more conservative than the recommended value $R - 1 < 0.1$.

3. Results

We summarize our main results in Table 1. For all the combined data (SN182 + WMAP3 + SDSS + 2dFGRS), we find that the flat universe is a good fit since the $\Omega_K = 0$ lies within the 68% region and $|\Omega_K| > 0.06$ has been excluded for more than 2σ for both DE parameterizations. This can be seen graphically in Fig. 1. From these 2D contour plots of energy density of dark energy and matter from different data combination and different DE parameterizations, we find that the data of supernova-only favor a non-flat universe, however when CMB and LSS data are combined, a flat universe is preferred.

For parametrization (I), we find the best fit value of (w_0, w_1) to be $(-1.149, 1.107)$ for a flat universe. When Ω_K is freely relaxed, the best fit value of (w_0, w_1) is changed to $(-1.053, 0.944)$ and the error bars of nearly all the cosmological parameters have been enlarged. We find dark energy models whose EoS can cross -1 are mildly favored.

The 1D posterior distribution of w_0, w_1, Ω_K and their 2D correlation are shown in Fig. 2. In the $w_0 - \Omega_K$ and $w_1 - \Omega_K$ panel, we find interesting correlation among curvature and DE parameters. This is expected since Ω_K can contribute to luminosity distance d_L via:

$$d_L(z) = \frac{1+z}{H_0 \sqrt{|\Omega_k|}} \, \text{sinn} \left[\sqrt{|\Omega_k|} \int_0^z \frac{dz'}{E(z')} \right], \tag{5}$$

$$E(z) \equiv \frac{H(z)}{H_0}$$

$$= \left[\Omega_m (1+z)^3 + \Omega_{\text{DE}} \exp \left(3 \int_0^z \frac{1 + w(z')}{1 + z'} dz' \right) \right.$$

$$\left. + \Omega_K (1+z)^2 \right]^{1/2}, \tag{6}$$

Table 1
Constraints of dark energy equation of state and some background parameters when relaxing Ω_K as a free parameter (left panel) and assuming a flat universe (right). For each case, we consider two forms of parametrization of dark energy EoS: linear ($w(a) = w_0 + w_1(1 - a)$) and oscillating ($w(a) = w_0 + w_1 \sin(w_2 \ln(a))$), set $w_2 = \frac{3}{2}\pi$, see text for explanation). Best fit models, which give the minimum χ^2, and the marginalized 1σ, 2σ errors are shown. All these constraints are from data combination of WMAP3 + SN182 + SDSS + 2dFGRS

	$w(a) = w_0 + w_1(1 - a)$					
	Ω_K free			$\Omega_K = 0$		
	Best fit	1σ	2σ	Best fit	1σ	2σ
Ω_K	-0.015	$[-0.024, 0.012]$	$[-0.058, 0.028]$	set to 0	set to 0	set to 0
w_0	-1.053	$[-1.204, -0.810]$	$[-1.441, -0.615]$	-1.149	$[-1.153, -0.807]$	$[-1.269, -0.606]$
w_1	0.944	$[-0.461, 0.957]$	$[-1.983, 1.223]$	1.017	$[-0.187, 0.972]$	$[-1.078, 1.163]$
Ω_m	0.282	$[0.262, 0.340]$	$[0.238, 0.423]$	0.291	$[0.264, 0.307]$	$[0.246, 0.332]$
	$w(a) = w_0 + w_1 \sin(w_2 \ln(a))$					
	Ω_K free			$\Omega_K = 0$		
	Best fit	1σ	2σ	Best fit	1σ	2σ
Ω_K	-0.012	$[-0.029, 3.5 \times 10^{-5}]$	$[-0.051, 0.015]$	set to 0	set to 0	set to 0
w_0	-1.614	$[-2.172, -1.037]$	$[-2.720, -0.660]$	-1.149	$[-1.940, -0.871]$	$[-2.454, -0.593]$
w_1	-1.046	$[-1.840, -0.162]$	$[-2.591, 0.557]$	-0.525	$[-1.718, -0.027]$	$[-2.508, 0.518]$
Ω_m	0.280	$[0.265, 0.333]$	$[0.240, 0.393]$	0.276	$[0.247, 0.292]$	$[0.230, 0.318]$

where $\mathrm{sinn}(\sqrt{|k|}x)/\sqrt{|k|} = \sin(x),\ x,\ \sinh(x)$ if $k = 1, 0, -1$. Furthermore, Ω_K can modify the angular diameter distance to
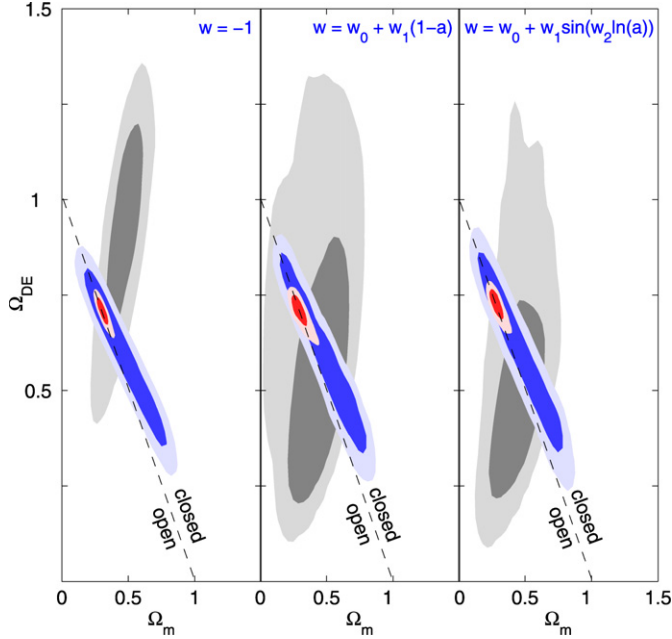

Fig. 1. 2D contour plots of energy density of matter and dark energy using latest astronomical observations. Grey: SN182; Blue: WMAP3; Red: WMAP3 + SN182 + SDSS + 2dFGRS. The dark and light shaded regions stand for 68% and 95% C.L., respectively. Different dynamical behaviors of dark energy have been considered. Left: vacuum energy ($w = -1$ forever); Middle: linearly growing ($w(a) = w_0 + w_1(1 - a)$); Right: oscillating ($w(a) = w_0 + w_1 \sin(w_2 \ln(a))$), with $w_2 = \frac{3}{2}\pi$. (For interpretation of the references to colour in this figure legend, the reader is referred to the web version of this Letter.)

last scattering surface and the transfer function, which leaves imprints on the CMB and matter power spectrum.

In the w_0–w_1 panel of Fig. 2, the parameter space has been divided into four parts. The upper right and lower left parts denote for $w > -1$ and $w < -1$, the regions for quintessence and phantom models, respectively. The other two parts dubbed "quintom A (B)" represent models whose EoS can cross -1 during evolution. Quintom A crosses -1 from upside down while quintom B transits -1 from the opposite direction. We also plot the results when assuming a flat universe for comparison. We see the best fit model is in the region of quintom A and the ΛCDM (the intersect of two dot dashed lines) is still a good fit. Moreover, relaxing Ω_K enlarges the $w_0 - w_1$ contour as expected.

For parametrization (II), again we find a small absolute value of Ω_K. The best fit models can cross -1 twice in the evolution. In Fig. 3, we show the correlation between Ω_K and dark energy parameters, and we find the quintom model whose EoS crosses -1 during evolution is preferred.

We can see the dynamics of dark energy more clearly from Fig. 4. We show the best fit model and 2σ errors of $w(z)$ for the case of flat universe and relaxing Ω_K as a free parameter for the two DE parameterizations. The best fit model of each case is quintom-like.

4. Summary and discussions

In this Letter we investigate the dynamics of dark energy and curvature of universe from the data of newly released 182 supernova data combined with CMB and LSS information. Rather
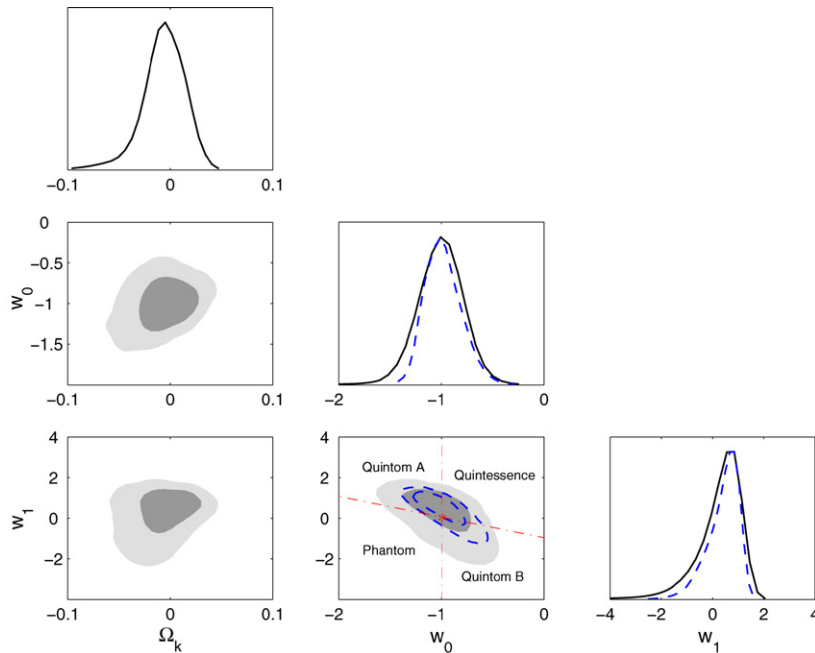

Fig. 2. Constraints on the curvature Ω_K and dark energy parameters w_0 and w_1 when parameterizing DE EoS as $w(a) = w_0 + w_1(1 - a)$. 1D plots show the posterior distribution of Ω_K, w_0 and w_1 while the 2D contour plots illustrate their correlation. The dark and light shaded area stand for 68% and 95% C.L., respectively. Blue dashed curves denote the case of flat universe for comparison. Different dark energy models can be distinguished from the $w_0 - w_1$ panel (see text). All these constraints are from data of WMAP3 + SN182 + SDSS + 2dFGRS. (For interpretation of the references to colour in this figure legend, the reader is referred to the web version of this Letter.)
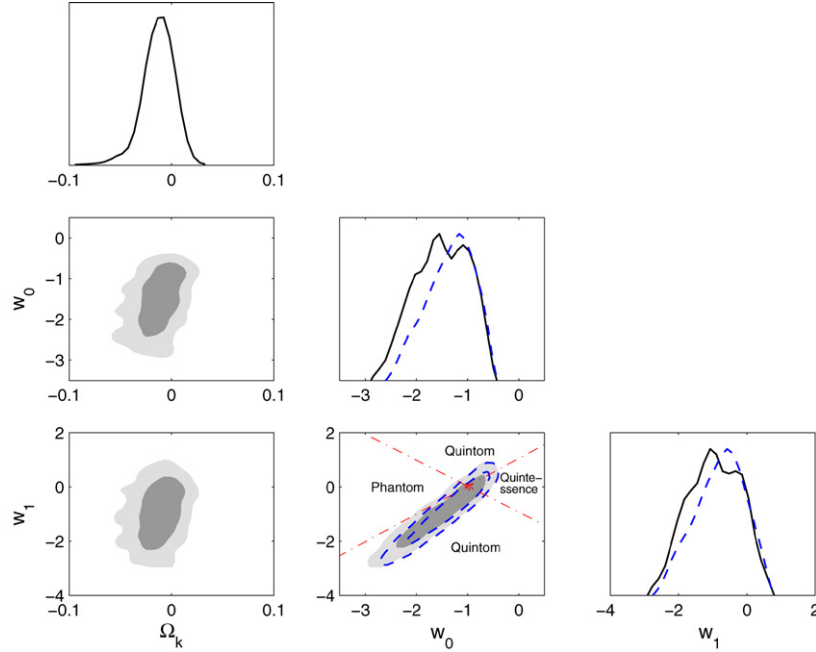
Fig. 3. The same graphic convention as in Fig. 2 except for the parametrization of the EoS of DE: $w(a) = w_0 + w_1 \sin(w_2 \ln(a))$. For simplicity, we have chosen w_2 to be $\frac{3}{2}\pi$. Note the variations of the error on Ω_k for negative Ω_k, as a function of w_1, which reflect the oscillating feature of this parametrization of the EoS.
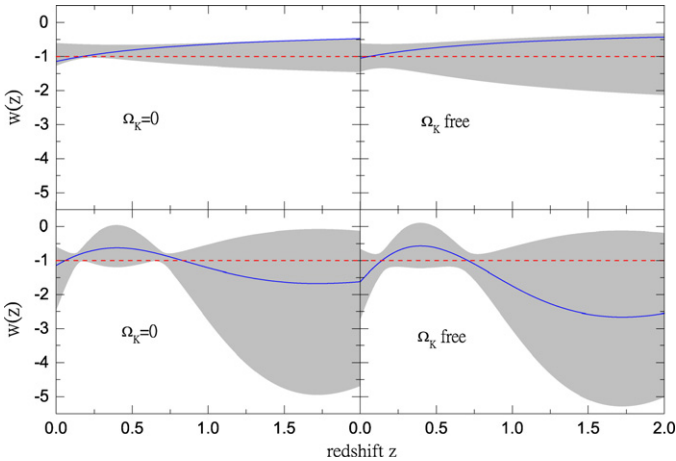

Fig. 4. Constraints of the time evolving of equation of state of DE using WMAP3 + SN182 + SDSS + 2dFGRS. Upper panel: $w(a) = w_0 + w_1(1-a)$; Lower panel: $w(a) = w_0 + w_1 \sin(w_2 \ln(a))$. The cases of flat universe and treating Ω_K as a free parameter are both considered as illustrated in the plot. The solid blue lines denote the best fit models while the shaded areas illustrate the 2σ errors. Red dashed lines show the cosmological constant boundary. (For interpretation of the references to colour in this figure legend, the reader is referred to the web version of this Letter.)

than assuming a flat universe, we relax Ω_K as a free parameter and make a MCMC global fit to measure the dark energy parameters as well as the curvature of universe. We find the model whose EoS can cross over -1 is favored for two dark energy parameterizations we considered in this work, albeit the ΛCDM model remains a good fit. A flat universe is preferred, namely, $\Omega_K = 0$ lies within the 68% region for two DE parameterizations and $|\Omega_K| > 0.06$ has been excluded by more than 2σ. However, the correlation among dark energy parameters and Ω_K might not be neglected. Freeing Ω_K enlarges the contours

and even modifies the best fit value of dark energy parameters. For example, for parametrization (II), relaxing Ω_K has changed the best fit value of (w_0, w_1) from $(-1.149, -0.525)$ to $(-1.614, -1.046)$. This is because adding Ω_K can reduce the total χ^2 by 1.2 thus the global minimum moves to a deeper point.

For CMB information, we use the full dataset of WMAP3, rather than the shift parameter. The shift parameter has the advantage of easy implementation and much shorter calculation time, but it is not really "model independent". It is derived from a fiducial ΛCDM model, thus it might lead to biased results, if one fits to models departing significantly from the fiducial model. Another drawback is that the shift parameter can merely offer part of the CMB information related to background parameters, thus it cannot constrain the perturbated dark energy.

The correlation between dark energy and spatial curvature has also been investigated by WMAP team [25] (see their Fig. 17). They took the equation of state of dark energy as a constant and derived $w = -1.062^{+0.128}_{-0.079}$ and $\Omega_K = -0.024^{+0.016}_{-0.013}$ at the 68% C.L. using CMB + 2dFGFS + SDSS + supernova data. Comparing their result and ours in Table 1, we find the flat universe is a good fit and the determination of Ω_K is slightly dependent on the parametrization of dark energy to some extent in that dark energy parameters are correlation with curvature as illustrated above.[4] For example, the 68% C.L. upper limit of Ω_K is -0.008 (result of WMAP team) and this quantity changes to 0.012 for linear parametrization and 3.5×10^{-5} for oscillating parametrization (our result).

---

[4] When comparing the WMAP result and ours, one should be aware that we use 182 SN data rather than 157 sample as WMAP group used.

We will have a deeper and deeper understanding of dark energy with the accumulation of high quality cosmological observation especially for supernova data, such as future SNAP, ESSENCE, etc. To be bias-free as much as possible, it is better to add Ω_K into the global analysis, use full datasets of CMB and carefully treat dark energy perturbation.

References

[1] A.G. Riess, et al., Astron. J. 116 (1998) 1009;
    S. Perlmutter, et al., Astrophys. J. 517 (1999) 565.
[2] R.R. Caldwell, E.V. Linder, Phys. Rev. Lett. 95 (2005) 141301;
    Z.K. Guo, Y.S. Piao, X. Zhang, Y.Z. Zhang, astro-ph/0608165.
[3] S. Weinberg, Rev. Mod. Phys. 61 (1989) 1;
    I. Zlatev, L.M. Wang, P.J. Steinhardt, Phys. Rev. Lett. 82 (1999) 896.
[4] B. Ratra, P.J.E. Peebles, Phys. Rev. D 37 (1988) 3406;
    P.J.E. Peebles, B. Ratra, Astrophys. J. 325 (1988) L17;
    C. Wetterich, Nucl. Phys. B 302 (1988) 668;
    C. Wetterich, Astron. Astrophys. 301 (1995) 321.
[5] R.R. Caldwell, Phys. Lett. B 545 (2002) 23.
[6] C. Armendariz-Picon, V. Mukhanov, P.J. Steinhardt, Phys. Rev. Lett. 85 (2000) 4438;
    C. Armendariz-Picon, V. Mukhanov, P.J. Steinhardt, Phys. Rev. D 63 (2001) 103510.
[7] G.B. Zhao, J.Q. Xia, M. Li, B. Feng, X. Zhang, Phys. Rev. D 72 (2005) 123515.
[8] J.Q. Xia, G.B. Zhao, B. Feng, H. Li, X. Zhang, Phys. Rev. D 73 (2006) 063521.
[9] J.Q. Xia, G.B. Zhao, B. Feng, X. Zhang, JCAP 0609 (2006) 015;
    G.B. Zhao, J.Q. Xia, B. Feng, X. Zhang, astro-ph/0603621.
[10] M. Tegmark, et al., astro-ph/0608632;
    U. Seljak, A. Slosar, P. McDonald, JCAP 0610 (2006) 014;
    U. Seljak, et al., SDSS Collaboration, Phys. Rev. D 71 (2005) 103515;
    M. Tegmark, et al., SDSS Collaboration, Phys. Rev. D 69 (2004) 103501.
[11] D. Huterer, A. Cooray, Phys. Rev. D 71 (2005) 023506;
    U. Alam, V. Sahni, A.A. Starobinsky, astro-ph/0612381;
    Y. Wang, M. Tegmark, Phys. Rev. Lett. 92 (2004) 241302;

[12] Y. Wang, M. Tegmark, Phys. Rev. D 71 (2005) 103513.
[12] V. Barger, Y. Gao, D. Marfatia, astro-ph/0611775.
[13] H. Li, M. Su, Z. Fan, Z. Dai, X. Zhang, astro-ph/0612060.
[14] B. Feng, X.L. Wang, X.M. Zhang, Phys. Lett. B 607 (2005) 35.
[15] H. Wei, R.G. Cai, hep-th/0501160;
    R.G. Cai, H.S. Zhang, A. Wang, hep-th/0505186;
    A.A. Andrianov, F. Cannata, A.Y. Kamenshchik, gr-qc/0505087;
    X. Zhang, astro-ph/0504586;
    Q. Guo, R.G. Cai, gr-qc/0504033;
    B. McInnes, Nucl. Phys. B 718 (2005) 55;
    E. Elizalde, S. Nojiri, S.D. Odintsov, P. Wang, Phys. Rev. D 71 (2005) 103504;
    I.Y. Aref'eva, A.S. Koshelev, S.Yu. Vernov, astro-ph/0507067;
    A. Anisimov, E. Babichev, A. Vikman, JCAP 0506 (2005) 006;
    H. Stefancic, astro-ph/0504518;
    J. Zhang, X. Zhang, H. Liu, astro-ph/0612642.
[16] X.F. Zhang, H. Li, Y.S. Piao, X.M. Zhang, Mod. Phys. Lett. A 21 (2006) 231;
    Z.K. Guo, Y.S. Piao, X.M. Zhang, Y.Z. Zhang, Phys. Lett. B 608 (2005) 177.
[17] M. Li, B. Feng, X.m. Zhang, JCAP 0512 (2005) 002;
    X.F. Zhang, T.T. Qiu, Phys. Lett. B 642 (2006) 187.
[18] H. Wei, R.G. Cai, Phys. Rev. D 73 (2006) 083002.
[19] B. Feng, M. Li, Y.S. Piao, X. Zhang, Phys. Lett. B 634 (2006) 101.
[20] J.Q. Xia, G.B. Zhao, H. Li, B. Feng, X. Zhang, Phys. Rev. D 74 (2006) 083521;
    J.Q. Xia, B. Feng, X.M. Zhang, Mod. Phys. Lett. A 20 (2005) 2409.
[21] J. Lesgourgues, S. Pastor, Phys. Rep. 429 (2006) 307;
    S. Hannestad, Phys. Rev. Lett. 95 (2005) 221301;
    J.Q. Xia, G.B. Zhao, X. Zhang, astro-ph/0609463.
[22] J.Q. Xia, G.B. Zhao, B. Feng, X. Zhang, JCAP 0609 (2006) 015.
[23] R.R. Caldwell, M. Kamionkowski, JCAP 0409 (2004) 009;
    K. Ichikawa, T. Takahashi, Phys. Rev. D 73 (2006) 083526;
    K. Ichikawa, M. Kawasaki, T. Sekiguchi, T. Takahashi, astro-ph/0605481;
    Z.Y. Huang, B. Wang, R.K. Su, astro-ph/0605392.
[24] A.G. Riess, et al., astro-ph/0611572.
[25] D.N. Spergel, et al., astro-ph/0603449.
[26] M. Chevallier, D. Polarski, Int. J. Mod. Phys. D 10 (2001) 213;
    E.V. Linder, Phys. Rev. Lett. 90 (2003) 091301.
[27] J. Weller, A.M. Lewis, Mon. Not. R. Astron. Soc. 346 (2003) 987.
[28] A. Lewis, S. Bridle, Phys. Rev. D 66 (2002) 103511;
    See also the CosmoMC website at: http://cosmologist.info.
[29] W.L. Freedman, et al., Astrophys. J. 553 (2001) 47.
[30] S. Burles, K.M. Nollett, M.S. Turner, Astrophys. J. 552 (2001) L1.
[31] For details see e.g. E. Di Pietro, J.F. Claeskens, Mon. Not. R. Astron. Soc. 341 (2003) 1299.
[32] M. Tegmark, et al., SDSS Collaboration, Astrophys. J. 606 (2004) 702.
[33] S. Cole, et al., 2dFGRS Collaboration, Mon. Not. R. Astron. Soc. 362 (2005) 505.
[34] M. Tegmark, et al., SDSS Collaboration, Phys. Rev. D 69 (2004) 103501.
[35] D.J. Eisenstein, et al., SDSS Collaboration, Astrophys. J. 633 (2005) 560.
[36] A. Gelman, D. Rubin, Stat. Sci. 7 (1992) 457.